Pergamon

0042-6989(94)00171-5

*Vision Res.* Vol. 35, No. 6, pp. 767–774, 1995

0042-6989/95 $9.50 + 0.00

# Neural Modulation Transfer Function of the Human Visual System at Various Eccentricities

JYRKI ROVAMO,* JUVI MUSTONEN,*† RISTO NÄSÄNEN†

*Received 21 January 1994; in revised form 14 July 1994*

**We measured r.m.s. contrast sensitivity as a function of retinal illuminance at various spatial frequencies within 3–37 deg of eccentricity in the nasal visual field. In dim light contrast sensitivity increased in proportion to the square root of retinal illuminance obeying the DeVries–Rose law but in bright light contrast sensitivity was independent of luminance following Weber's law. Critical retinal illuminance ($I_c$) marking the transition between the laws was found to be independent of grating area but proportional to the spatial frequency squared at all eccentricities, in agreement with the Van Nes–Bouman law of foveal vision. In addition, the proportionality constant was found to be independent of eccentricity and similar to that of the fovea. According to our contrast detection model of human vision the modulation transfer function ($P_{MTF}$) of the neural visual pathways squared is directly proportional to the critical retinal illuminance. On this basis our result means that $P_{MTF}$ is similar, i.e. equal to spatial frequency across the visual field, thus attenuating low spatial frequencies relatively more than high spatial frequencies. Hence, up to the spatial cut-off frequency determined by the lowest neural sampling density of each retinal location the neural modulation transfer function is independent of visual location.**

Modulation transfer function  Neural visual pathways  Contrast sensitivity  Retinal illuminance  Eccentricity

## INTRODUCTION

Human increment thresholds obey Weber's law in bright light but DeVries–Rose law (Rose, 1942; DeVries, 1943) in dim light. Performance at intermediate light levels falls between DeVries–Rose and Weber's laws (Kelly, 1972; Koenderink, Bouman, Bueno de Mesquita & Slappendel, 1978; Savage & Banks, 1992). The two laws mean that at higher levels of retinal illuminance contrast sensitivity is independent of light level but at lower levels of retinal illuminance contrast sensitivity for gratings is directly proportional to the square root of the average luminance (Van Nes & Bouman, 1967; Mustonen, Rovamo & Näsänen, 1993).

Transition from Weber's to DeVries–Rose law is determined by spatial frequency so that the lower the spatial frequency, the lower the retinal illuminance where the transition occurs (Van Nes & Bouman, 1967). According to the Van Nes–Bouman law the transition luminance is in fact directly proportional to spatial frequency squared (Van Nes, Koenderink, Nas & Bouman, 1967; Mustonen *et al.*, 1993).

On the basis of the experiments of Koenderink *et al.* (1978) performed with a 1 c/deg moving grating, foveal contrast sensitivity decreases when retinal illuminance decreases from 10 to 0.1 phot td whereas peripheral contrast sensitivity remains independent of retinal illuminance within 0.1–10 phot td. This suggests that for the same spatial frequency and range of retinal illuminance the periphery is in the Weber region whereas fovea is in the DeVries–Rose region. One possible explanation for the finding that peripheral contrast sensitivity remains independent of retinal illuminance within 0.1–10 phot td is transition from cone to rod vision. An alternative explanation for the difference between the fovea and periphery could be that critical retinal illuminances are lower in the peripheral than foveal vision either (i) because the proportionality constant between $I_c$ and spatial frequency squared decreases with increasing eccentricity; or (ii) because the dependence of $I_c$ on spatial frequency is otherwise different in the foveal and peripheral vision. Koenderink *et al.* (1978) explained their finding by the fact that the receptive fields of ganglion cells are larger in the peripheral than foveal vision and therefore collect more light quanta and are consequently more light adapted at the same level of retinal illuminance (Enroth-Cugell & Shapley, 1973).

The purpose of this paper was thus to study systematically the effect of retinal illuminance on contrast sensitivity across the visual field by using stationary cosine gratings of various spatial frequencies. Our second aim

*Department of Vision Sciences, Aston University, Aston Triangle, Birmingham B4 7ET, England.
†Institute of Biomedicine, Department of Physiology, P.O. Box 9 (Siltavuorenpenger 20 J), SF-00014 University of Helsinki, Finland.

was to find out the relationship between $I_c$ and spatial frequency at different locations, because according to our model (Rovamo, Mustonen & Näsänen, 1994) the modulation transfer function ($P_{MTF}$) of the neural visual pathways is proportional to the square root of $I_c$.

## MODELLING THE RELATIONSHIP BETWEEN $P_{MTF}$ AND $I_c$

Visual stimuli are filtered by the ocular optics and neural visual pathways before being interpreted by the human brain. We have recently modelled this sequence as a simple image processor comprising (i) low-pass filtering due to the optical modulation transfer function of the eye; (ii) addition of light-dependent noise at the event of quantal absorption; (iii) high-pass filtering due to the modulation transfer function of the neural visual pathways; (iv) addition of internal neural noise; and (v) detection by a local matched filter whose efficiency decreases with increasing grating area.

Retinal illuminance ($I$) is directly proportional to the effective luminous flux (photons $\text{deg}^{-2}\,\text{sec}^{-1}$) absorbed in the outer segments of photoreceptors. Effective luminous flux ($F$) is inevitably smaller than the external luminous flux entering the eye through the pupil, as some light is absorbed before it reaches the photoreceptors and even there only part of the remaining light is absorbed. According to Pelli (1990) the effective luminous flux is equal to the inverse of the spectral density of quantal noise ($N_q$). Thus, on the basis of the above,

$$I = KF = KN_q^{-1}, \quad (1)$$

where $K$ is constant.

According to the detection model of human visual system (Rovamo et al., 1994)

$$S = S_{max}(1 + I_c/I)^{-0.5}, \quad (2)$$

where $S$ is r.m.s. contrast sensitivity, $S_{max}$ is the maximum contrast sensitivity obtainable in bright light for the stimulus used, $I$ is photopic retinal illuminance, and $I_c$ is the critical retinal illuminance marking the transition between DeVries–Rose and Weber's laws. The equation means, that at high luminance levels $S = S_{max}$. (i.e. independent of luminance level) as Weber's law predicts. At luminance levels below $I_c$, r.m.s. contrast sensitivity obeys the DeVries–Rose law decreasing in proportion to the square root of decreasing retinal illuminance. Equation (2) applies to all grating areas, because the effect of spatial integration is taken into account by allowing $S_{max}$ to grow with area.

According to equation (2) contrast sensitivity becomes reduced to $S_{max}/\sqrt{2}$ when illuminance is reduced to $I_c$. By definition contrast energy threshold is proportional to $S^{-2}$. Hence, at $I = I_c$ the contrast energy threshold is twice its minimum value obtainable in bright light. The doubling of contrast energy threshold due to quantal noise at $I = I_c$ means that the effect of critical spectral density of quantal noise ($N_{qc}$) corresponding to $I_c$ is equivalent to the effect of additive internal neural noise ($N_i$).

In fact, $N_{qc}$ transferred through the ocular optics and neural visual pathways is equal to $N_i$. However, the spectral density of quantal noise corresponding to $I_c$ is only filtered by the neural modulation transfer function ($P_{MTF}$) of the visual pathways but left unaffected by the optical modulation transfer function of the eye because individual light quanta cannot be blurred by the point spread function of ocular optics (Rovamo et al., 1994). In other words, although ocular optics redistributes light so that high spatial frequencies in the image are attenuated more than low spatial frequencies, optics does not introduce correlations among neighbouring points, and therefore it does not attenuate the high spatial frequencies of quantal noise (Graham & Hood, 1992). Thus,

$$P_{MTF}^2(f)N_{qc} = N_i, \quad (3)$$

where $f$ is spatial frequency.

On the basis of equation (1) we can write equation (3) as

$$P_{MTF}^2(f) = (N_i/K)I_c, \quad (4)$$

which means that $I_c$ is only affected by the neural visual pathways. Thus, $I_c$ remains independent of optical blur although contrast sensitivity at high spatial frequencies and in peripheral vision is reduced by ocular optics.

For foveally viewed cosine gratings $I_c$ is directly proportional to spatial frequency squared (Van Nes et al., 1967; Mustonen et al., 1993). Hence, on the basis of equation (4) the foveal $P_{MTF}$ for cosine gratings is proportional to spatial frequency, confirming the finding of Rovamo, Luntinen and Näsänen (1993a). Thus, cosine gratings are relatively more attenuated at low than high spatial frequencies by the foveal $P_{MTF}(f)$.

For the sake of simplicity and without losing generality Rovamo et al. (1993a) assumed that $P_{MTF}(f) = f$ at the fovea. According to the foveal experiments of Rovamo et al. (1994) $I_c = I_o f^2$, where the numerical value of $I_o$ provides an estimate for $I_c$ at 1 c/deg. Thus, $(N_i/K) = I_o^{-1}$ in equation (4).

## METHODS

*Apparatus*

The apparatus has been described in detail in Rovamo, Kukkonen, Tiippana and Näsänen (1993b). Therefore only its main features are described here.

Sinusoidal vertical gratings were generated under computer control on a high resolution 16 in. RGB monitor driven at the frame rate of 60 Hz by a VGA graphics board that generated 640 × 480 pixels. The pixel size was $0.42 \times 0.42\ \text{mm}^2$ on the screen. The display was used in a white mode. The average photopic luminance of the display was measured with a Minolta Luminance Meter LS-110. It was set to $50\ \text{cd/m}^2$, corresponding to a scotopic luminance of $130\ \text{cd/m}^2$, measured with a Bentham PMC 3B spectroradiometer. The CIE 1931 $(x, y)$ chromaticity coordinates, measured with the spectroradiometer, were (0.30, 0.31). The non-linear luminance response of the display was linearised by using the inverse function of the luminance response when computing the stimulus images. The contrast of simple cosine gratings was independent of orientation and spatial frequency up to 2 c/cm on the screen.

A monochrome signal of 1024 intensity levels (10 bits) from a monochrome palette of 65,536 (16 bits) intensity levels was obtained by means of a video summation device (Pelli & Zhang, 1991) and a periodic dither signal (Näsänen, Kukkonen & Rovamo, 1993). In our experiments the dither was completely invisible, because its contrast was about 0.007 when the contrast of the grating was equal to 1 and decreased to 0.0001 at the lowest grating contrasts. The lowest spatial frequency component of the dither was 12 c/cm, which is over 2.5 octaves above the spatial frequency of the gratings at 2 c/cm. This guarantees that the dither had no masking effects. The 10 bit signal within the range of 16 bits allowed the measurement of contrast sensitivity with simple cosine gratings consisting of about 50 different grey levels even at a Michelson contrast as low as 0.00125. Michelson contrasts of the simple cosine gratings used for measurements at and above 0.1% were checked with the Minolta Luminance Meter LS-110.

*Stimuli*

The stimuli consisted of vertical cosine gratings within sharp-edged circular apertures. Equally well we could have chosen a square aperture, because the shape or the phase at which contrast is abruptly reduced to zero has no effect on contrast sensitivity (Rovamo *et al.*, 1993a). The apertures used were 2–16 cm in diameter. Spatial frequencies were 2 and 0.5 c/cm on the screen. The equiluminous surround was limited to a circular aperture of 20 cm in diameter by a black cardboard.

The stimuli were created and experiments were run by means of a software developed by one of the authors (RN). For further details see Rovamo *et al.* (1993b). The software utilized the graphics subroutine library of a Professional HALO 2.0 developed by Media Cybernetics. The grating contrast was changed in steps of 0.1 $\log_{10}$ units. The stimulus was rapidly switched on and off by changing the colour look-up table during the vertical retrace period of the display.

Contrast energies of gratings were calculated by integrating the contrast waveform $c(x, y)$ numerically across the grating area:

$$E = \Sigma\,\Sigma\, c^2(x, y)p^2, \tag{5}$$

where $c(x, y) = [L(x, y) - L_o]/L_o$, $L(x, y)$ is the luminance distribution of the grating, $L_o$ is the luminance averaged across the equiluminous screen, and $p^2$ is the area of a pixel in solid degrees of the visual field. Thus, for each pixel the deviation of luminance from the average luminance was first divided by the average luminance to obtain a measure of local contrast. These measures were then squared and multiplied by pixel area. Their sum then indicates the contrast energy. The r.m.s. contrast was thereafter calculated as

$$c_{\text{r.m.s.}} = \sqrt{(E/A)}, \tag{6}$$

where $A$ is grating area. The r.m.s. contrast is thus equal to the standard deviation of luminance distribution calculated pixel by pixel across the grating area and divided by the average luminance. For simple cosine gratings the r.m.s. contrast is equal to Michelson contrast divided by $\sqrt{2}$. Michelson contrast is defined as $(L_{\max} - L_{\min})/(L_{\max} + L_{\min})$, where $L_{\max}$ and $L_{\min}$ are the maximum and minimum luminances of the simple cosine grating.

*Procedures*

After installing one drop of 0.4% benoxinate (Oxybuprocaine) hydrochloride to increase drug absorption, the pupil of the dominant eye was dilated to 8 mm with 2 drops of 10% phenylephrine (Metaoxedrine) hydrochloride. Both drugs were obtained from single use disposable units (Smith & Nephew Pharmaceuticals Ltd, Romford, England). Metaoxedrine leaves accommodation unaffected. The other eye was covered by a black eye pad. The grating stimuli were thus viewed monocularly.

Monocular fixation to a small target does not necessarily guarantee an accurate accommodative response. The resulting blur would then reduce contrast sensitivity at high spatial frequencies. However, by using 0.5% cyclopentolate hydrochloride that both dilates pupil and paralyzes accommodation we have shown (Rovamo *et al.*, 1994) that contrast sensitivity at 16 c/deg is no better with optimal refraction than natural accommodation.

The average retinal illuminance produced by our display through a pupil with 8 mm diameter was 2500 phot td, corresponding to 6500 scot td. Lower levels of retinal illuminance were obtained by placing a desired number of neutral density filters (Lee Filters Ltd, Hampshire, England) of 0.6 log units (No. 210 ND) on the screen. The filters were fixed by black opaque tape that prevented leakage of light from between the filters and screen. Filters of suitable size were cut from large sheets. Each filter used was calibrated by measuring how much it attenuated the luminance of the screen. After each luminance reduction of 0.6 log units, the subject adapted to the new screen luminance for 5 min.

Contrast sensitivity is the inverse of r.m.s. contrast at threshold. The contrast thresholds were determined by a two-alternative forced-choice algorithm with four-correct-then-down/one-wrong-then-up rule. For further details see Mustonen *et al.* (1993). Each trial consisted of two 500 msec exposures, separated by about 600 msec. Both exposures contained the grating stimulus and were accompanied by a sound signal. However, only one exposure contained a stimulus with non-zero contrast; in the other the contrast was always zero. Between the two exposures and during the inter-trial intervals the observer saw only the equiluminous field. A new trial began 250 msec after the observer's response. She/he indicated which exposure contained the grating by pressing one of the two keys on a computer keyboard. A wrong choice was followed by another sound signal to provide feedback about the correctness of the response.

The threshold contrast required for the probability of 0.84 correct was estimated as an arithmetic mean of the last eight reversal contrasts (Wetherill & Levitt, 1965). All data points shown are medians of at least three threshold estimates. The experiments were performed in a dark room, the only light sources being the display and a self-luminous fixation point. Eccentricity within 3–37 deg refers to the angular distance between the point of fixation and the centre of the grating in the nasal visual field of the dominant eye. Thus, at the eccentricity of 37 deg the nearest edge of the largest grating was at the distance of 21 deg from the fovea. The stimulus field was always perpendicular to the line determined by the pupil and the centre of the grating. Both the fixation point and grating were always at the same viewing distance from the eye. Subject's head was stabilized using a chin rest. A small black dot served as a fixation point within the luminous screen, and a small, red LED—whose luminance was reduced by neutral density filters in accordance with the screen luminance—served as a fixation point outside the screen.

*Subjects*

Four experienced subjects, aged 23–31 yr, served as observers. All were corrected myopes: refractions in the dominant eye were TH (o.d.), −1.75 D; KL (o.d.), −1.75 cyl, −0.5 ax 90 deg; JM (o.d.), −0.75 cyl, −0.25 ax 90 deg; and SU (o.d.), −4.0 D. Their accommodation had a range of at least 6 D. Hence, they were emmetropes at the viewing distances of 28.6–229 cm used in our experiments. With optimal refraction their monocular Snellen acuities at 5 m were within 1.2–1.6.

## RESULTS

In the foveal vision the increase and saturation of contrast sensitivity as a function of retinal illuminance is similar for all grating areas (Rovamo *et al.*, 1994). Thus, the critical illuminance ($I_c$) marking the transition between the increasing and saturated parts of the contrast sensitivity function is independent of grating area in the foveal vision. According to our contrast detection model of human vision (Rovamo *et al.*, 1994) $I_c$ should be independent of grating area also in peripheral vision.

To test the above hypothesis we measured in Fig. 1 contrast sensitivity as a function of retinal illuminance for various grating areas at the eccentricity of 37 deg in the nasal visual field. Retinal illuminance varied across 4 log units from $3.83 \times 10^{-2}$ to $6.28 \times 10^{2}$ phot td. Retinal illuminance is not affected by eccentricity because the retinal area per 1 solid degree of visual field and the effective pupillary area decrease similarly when eccentricity increases from 0 to 80 deg (Bedell & Katz, 1982; Rovamo, 1983). Spatial frequency was 1 c/deg. Test grating areas covered a range from 12.6 to 804 deg$^2$. Consequently the number of square cycles ($Af^2$) (Virsu & Rovamo, 1979), calculated by multiplying grating area ($A$) by spatial frequency ($f$) squared, ranged from 12.6 to 804.

As Fig. 1 shows, contrast sensitivity increased with retinal illuminance at all grating areas. The slope of increase was 0.5 at low levels of retinal illuminance, obeying the DeVries–Rose law (Rose, 1942; DeVries, 1943). The increase then saturated at high levels of retinal illuminance and contrast sensitivity became independent of luminance level, obeying Weber's law. Scrutiny of the data revealed that critical illuminance was independent of grating area, because the contrast sensitivity functions measured in Fig. 1 were parallel at all grating areas.

The contrast sensitivity functions of Fig. 1 were first averaged in vertical direction across grating areas at 0.15–39 phot td. Equation (2) was then fitted to this geometrical average with the method of least squares (see Appendix) in order to obtain the value for $I_c$. It was found to be 5.3 phot td. Thereafter, on the basis of equation (2), the r.m.s. contrast sensitivity values measured for each grating area at various levels of retinal illuminance were first divided by the corresponding values of expression $(1 + I_c/I)^{-0.5}$ and then geometrically averaged in order to get the estimates of $S_{max}$ for the grating areas used in Fig. 1. They were found to be 16.5, 36.9, 57.3, and 93.3 for areas of 12.6, 50.3, 201, and 804 deg$^2$, respectively. Smooth curves in Fig. 1 were then calculated by equation (2) fitted to the data of each grating area separately. Explained variance, calculated by equation (A3) in the Appendix, was 98%, when $S_{max}$ was allowed to vary with grating area.

In the experiments of Fig. 2 we extended our studies

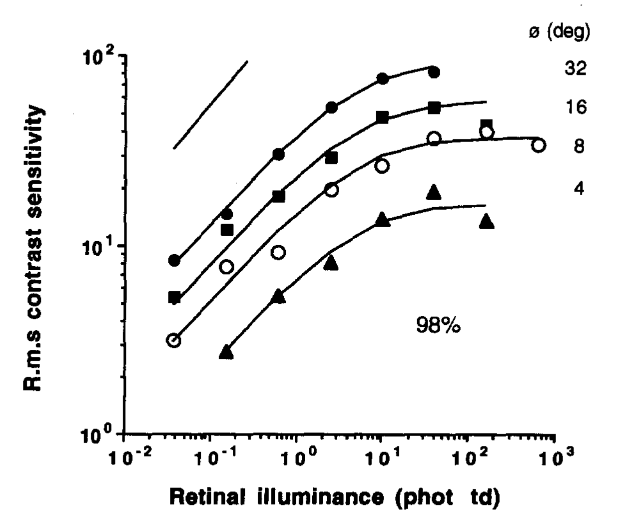


FIGURE 1. Monocular contrast sensitivity as a function of retinal illuminance at 1 c/deg for vertical cosine gratings at the eccentricity of 37 deg. Spatial frequency was 2 c/cm on the screen. Grating diameters were 2, 4, 8, and 16 cm, corresponding to 4–32 cycles. Smooth curves have been calculated by equation (2) fitted to the data. The explained percentage of the total variance, calculated by equation (A3), indicates the goodness of the fit. Even the largest grating diameter at the viewing distance of 28.6 cm was calculated in deg by assuming that 0.5 cm = 1 deg, because this assumption kept the comparison between the diameters and number of cycles very simple. Viewing distance was 28.6 cm, subject was JM.

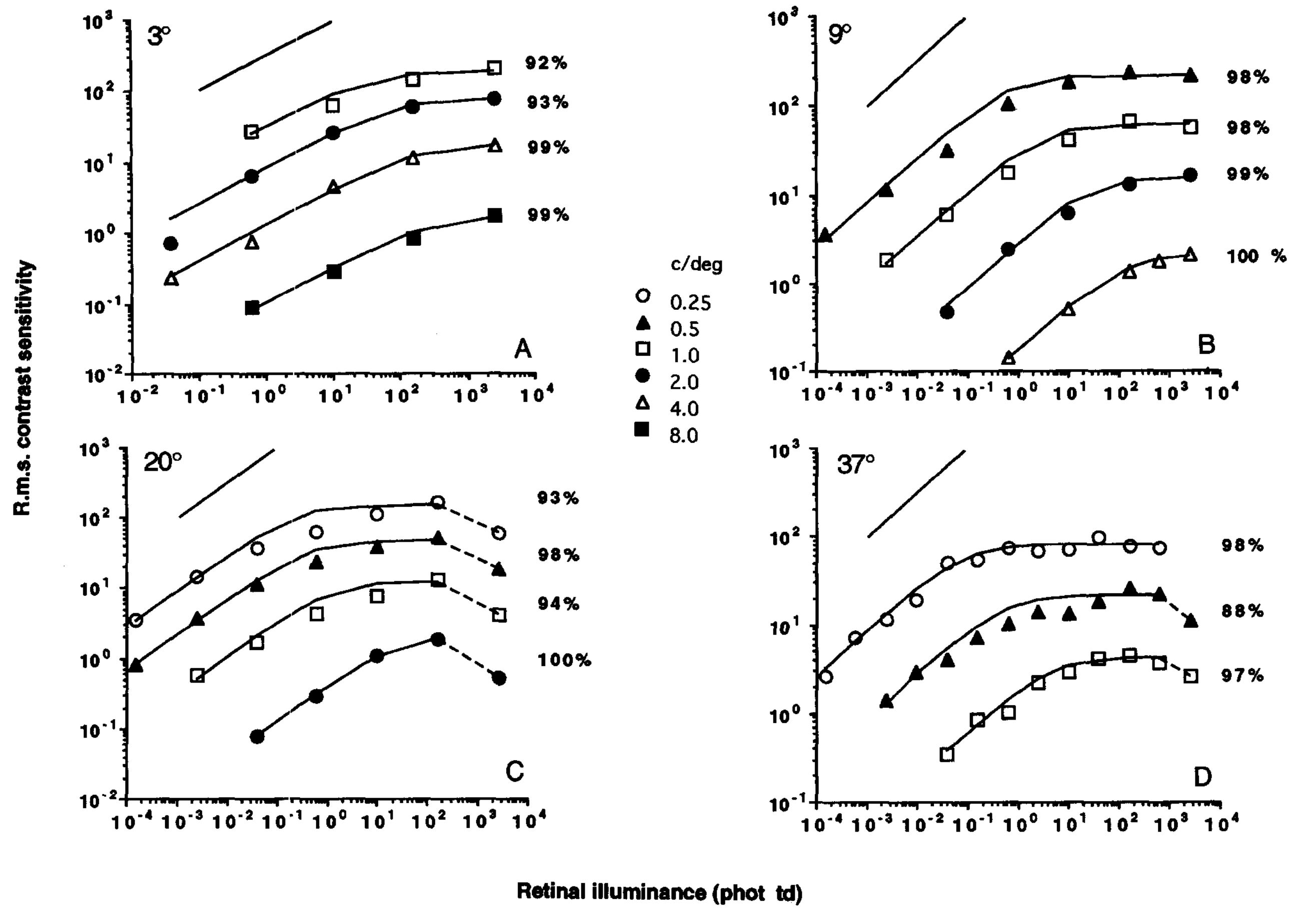


FIGURE 2. Monocular contrast sensitivity as a function of retinal illuminance at spatial frequencies of 0.25–8 c/deg (in octave steps) for vertical cosine gratings at eccentricities of 3, 9, 20, and 37 deg in the nasal visual field. Grating diameters were 4 and 16 cm for spatial frequencies of 2 and 0.5 c/cm on the screen. Smooth curves have been calculated by equation (2) fitted to the data. The explained percentage of the total variance, calculated by equation (A3) for each curve, indicates the goodness of the fit. For the clarity of presentation the curves and data points have been shifted vertically. In each frame the uppermost curve and data are in their correct place but the others have been shifted downwards by a factor of 3, 9, and 27, respectively. The angular diameter of the circular grating window varied inversely with spatial frequency so that eight cycles were presented at all spatial frequencies. (A) Eccentricity was 3 deg. Viewing distance was 114 cm for 1 and 4 c/deg but 229 cm for 2 and 8 c/deg. Subject was KL. (B) Eccentricity was 9 deg. For 0.5 and 2 c/deg viewing distance was 57.3 cm and subject JM. For 1 and 4 c/deg viewing distance was 114 cm and subject TH. (C) Eccentricity was 20 deg. Viewing distance was 28.6 cm for 0.25 and 1 c/deg but 57.3 cm for 0.5 and 2 c/deg. Subject was SU. (D) Eccentricity was 37 deg. Viewing distance was 28.6 cm for 0.25 and 1 c/deg but 57.3 cm for 0.5 c/deg. Subject was JM. The data for 1 c/deg up to $6.28 \times 10^2$ phot td is replotted from Fig. 1.

to other spatial frequencies and eccentricities in the nasal visual field and measured monocular, r.m.s. contrast sensitivity as a function of retinal illuminance for vertical cosine gratings. The spatial frequencies used were 0.25–8 c/deg at 3–37 deg of eccentricity. The number of square cycles ($Af^2$) was constant at 50. The upper limit of the spatial frequencies studied at each eccentricity was determined by the local grating acuity, and the lower limit of the spatial frequencies studied was determined by the largest grating area available on the screen and the shortest practical viewing distance. Retinal illuminance varied across 8 log units from $1.50 \times 10^{-4}$ to $2.51 \times 10^3$ phot td.

As Fig. 2 shows, contrast sensitivity increased with retinal illuminance at all spatial frequencies and eccentricities studied. The slope of increase was again 0.5 at lower levels of retinal illuminance, obeying the DeVries–Rose law. The increase then saturated at higher levels of retinal illuminance and contrast sensitivity became independent of luminance level, obeying Weber's law. In addition, above 160–630 phot td. contrast sensitivity at the eccentricities of 20–37 deg decreased with increasing retinal illuminance. The decrease was also found at the eccentricity of 37 deg in the experiments of Fig. 1 above 39–630 td (not shown). In addition, Daitch and Green (1969) reported a similar phenomenon for 0.5–1 c/deg at the eccentricity of 12 deg in the nasal visual field.

From Fig. 2 it can be seen that the critical retinal illuminance marking the transition between De Vries–Rose and Weber's laws increased with spatial frequency, in agreement with Van Nes and Bouman (1967) and Mustonen *et al.* (1993). Scrutiny of the data also showed that at low spatial frequencies ($\leqslant 1$ c/deg) performance often fell between DeVries–Rose and Weber's laws at intermediate light levels, in agreement with Kelly (1972), Koenderink *et al.* (1978), and Savage and Banks (1992).

Equation (2) was first fitted separately to the data of each spatial frequency at each eccentricity with the method of least squares. Smooth curves in Fig. 2 were then calculated by using equation (2) with corresponding parameters. The data points where contrast sensitivity decreases with increasing retinal illuminance were excluded from the least squares regression. Explained variance, calculated by equation (9), was on average 96%, with a range of 88–100% across spatial frequencies and eccentricities.

In Fig. 3(A) the estimates of critical retinal illuminance ($I_c$) marking the transition between the DeVries–Rose and Weber's laws were plotted as a function of spatial frequency in double logarithmic coordinates. The estimates of $I_c$ at 3–37 deg of eccentricity were obtained when equation (2) was fitted to the data of Fig. 2 whereas the foveal estimates of $I_c$ were obtained from our previous study (Rovamo *et al.*, 1994).

As Fig. 3(A) shows, all the estimates of critical retinal illuminance fell on a common straight line and in double logarithmic coordinates $I_c$ increased linearly with spatial frequency of 0.125–32 c/deg. The deviations of the estimates of $I_c$ from the straight line are similar in magnitude to those found for monochromatic foveal gratings (see Laming, 1991). However, the fact that our data has been collected from eight subjects at various spatial frequencies and eccentricities could contribute to the variability of $I_c$ values across eccentricities at each spatial frequency. The slope of increase was 2, which means that $I_c$ increased in direct proportion to spatial frequency squared, in agreement with the foveal results of Van Nes *et al.* (1967) and Mustonen *et al.* (1993). This also means that critical retinal flux, calculated by dividing critical retinal illuminance by spatial frequency squared (Mustonen *et al.*, 1993), was constant at all spatial frequencies and eccentricities. The straight line $I_c = I_o f^2$ in Fig. 3(A) is a least-squares fit to the data. The explained variance was 93%. The value of constant $I_o$ was found to be 5.22 phot td. deg$^2$, in agreement with Fig. 1. It is also an estimate for the critical retinal flux at all spatial frequencies and eccentricities.

In Fig. 3(B) we plotted $(I_c/I_o)^{0.5}$ as a function of spatial frequency, because according to equation (4) $P_{MTF} = (I_c/I_o)^{0.5}$. As Fig. 3(B) shows $P_{MTF} = f$ provided good fit to the data. Explained variance was 93%.

## DISCUSSION

Our experiments showed that for cosine gratings the increase of contrast sensitivity with retinal illuminance was similar at all eccentricities in the nasal visual field. Contrast sensitivity increased in proportion to the square root of retinal illuminance ($I$) in dim light, thus obeying the DeVries–Rose law, but was independent of retinal illuminance in bright light, following Weber's law. The dependence of r.m.s. contrast sensitivity ($S$) on retinal illuminance was quantitatively described by equation (2) at all spatial frequencies. The explained variance was 96% on the average, and had a range of 88–100% across spatial frequencies and eccentricities. In equation (2) $S_{max}$ is the maximum contrast sensitivity obtainable in bright light at the exposure duration and grating area used, and $I_c$ is the critical retinal illuminance marking the transition between DeVries–Rose and Weber's laws.

At low spatial frequencies performance fell between De Vries–Rose and Weber's laws at intermediate light levels, in agreement with Kelly (1972), Koenderink *et al.* (1978), and Savage and Banks (1992). One explanation for the slow transition from Weber's to DeVries–Rose law with decreasing luminance is the fact that the increase in the effective spectral density of quantal noise with decreasing luminance is retarded by the increasing quantum efficiency that is due to transition from cone to rod vision. This slow transition between De Vries–Rose and Weber's laws at low spatial frequencies was not predicted by our model. The quantitative differences

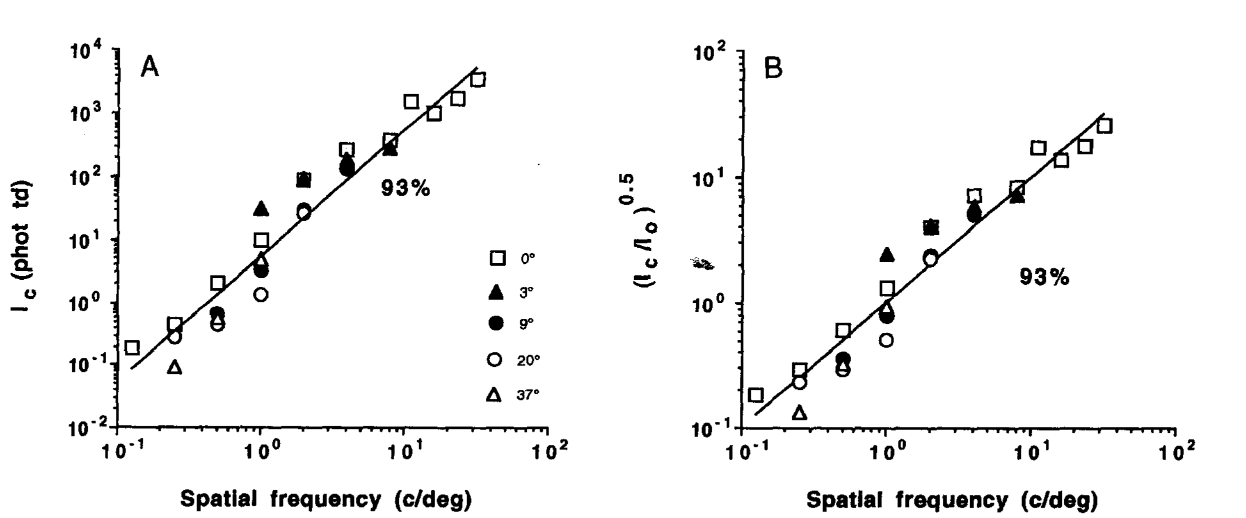


FIGURE 3. The estimates of critical retinal illuminance ($I_c$) plotted as a function of spatial frequency. The solid line was calculated by the equation $I_c = I_o f^2$ fitted to the estimates of $I_c$. The extrafoveal estimates of $I_c$ were obtained by fitting equation (2) to the data of Fig. 2 at each spatial frequency and eccentricity. The foveal estimates of $I_c$ were obtained from Rovamo *et al.* (1994). (B) The relation between $P_{MTF}$ and spatial frequency. According to equation (4) $P_{MTF}(f) = (I_c/I_o)^{0.5}$. The solid line refers to equation $P_{MTF}(f) = f$. The explained variance indicates the goodness of fit.

between predicted and measured contrast sensitivities were, however, small, because explained variance remained high at 88–98% even at low spatial frequencies.

Analysis of our experimental data revealed that at all eccentricities and spatial frequencies studied, the critical retinal luminance $I_c$ was directly proportional to spatial frequency squared, i.e. $I_c = I_o f^2$, where $I_o = 5.22$ phot td deg$^2$ and $f$ is spatial frequency in c/deg. Explained variance was 93%. The finding means that our study extends the foveal result of Van Nes *et al.* (1967) and Mustonen *et al.* (1993) throughout the visual field. The value of $I_o$, calculated by dividing critical retinal illuminance ($I_c$) by spatial frequency squared, indicates the critical retinal flux 5.22 phot td deg$^2$ that is valid for all spatial frequencies and eccentricities. Thus, the previous foveal result that the transition between DeVries–Rose and Weber's laws takes place at the same retinal flux irrespective of spatial frequency (Mustonen *et al.*, 1993) was generalized across the whole visual field.

Koenderink *et al.* (1978) concluded that the far retinal periphery is less affected by a decrease in the retinal illuminance than the foveal region so that at the same spatial frequency the transition point between De Vries–Rose and Weber's laws is lower for a peripheral grating. This clearly disagrees with our findings. However, Koenderink *et al.* (1978) used moving gratings, whose size was larger in the periphery than at the fovea. Based on a previous foveal investigation (Rovamo *et al.*, 1994) and on the results of the present study (Fig. 1), it appears that critical retinal illuminance is independent of stimulus area for stationary gratings. Therefore, the probable reason for the discrepancy between our results and the finding of Koenderink *et al.* (1978) is grating movement.

Daitch and Green (1969) used gratings exposed for 0.2 sec at the eccentricity of 12 deg and measured contrast sensitivity as a function of retinal illuminance below 30 phot td for several spatial frequencies. Their contrast sensitivities were lower than those found at the eccentricity of 9 deg in the current study probably because of their short exposure duration. We fitted equation (2) to their data at 0.5–4 c/deg and found that critical retinal illuminance was proportional to spatial frequency squared with an explained variance of 79%.

In bright light visual acuity for symbols is far better (Mandelbaum & Sloan, 1947) and gratings are resolved at higher spatial frequencies (Rovamo & Raninen, 1990) in the fovea than periphery. Both visual acuity and grating resolution decrease with retinal illuminance but the reduction starts in the fovea at higher luminance levels than in the periphery (Mandelbaum & Sloan, 1947; Rovamo & Raninen, 1990). This phenomenon is conventionally explained by assuming that the fovea enters the DeVries–Rose region at higher luminance levels than the retinal periphery (Koenderink *et al.*, 1978). However, according to our results high spatial frequencies enter the DeVries–Rose region at higher luminance levels than low spatial frequencies irrespective of retinal location, thus explaining the dependence of acuity on retinal illuminance and eccentricity.

All the equations used to fit and analyse the data were derived from our contrast detection model of human vision (Rovamo *et al.*, 1994). According to the model the modulation transfer function ($P_{MTF}$) of the neural visual pathways squared is directly proportional to critical retinal illuminance ($I_c$) at all spatial frequencies. Hence, our finding that $I_c$ was similarly proportional to spatial frequency squared at all eccentricities means that up to the spatial cut-off frequency determined (Rovamo & Virsu, 1979) by the lowest local sampling density (cones at eccentricities 0–10 deg and ganglion cells above 10 deg) the modulation transfer function ($P_{MTF}$) of the neural visual pathways is similar (i.e. equal to spatial frequency) at all visual field locations. Hence, according to our model the decrease of contrast sensitivity with increasing eccentricity at high spatial frequencies is due to deterioration in ocular optics or spatial summation. The latter alternative is supported by Banks, Sekuler and Anderson (1991), who concluded that the neural efficiency of detection at high spatial frequencies decreases with increasing eccentricity.

## REFERENCES


Banks, M. S., Sekuler, A. B. & Anderson, J. S. (1991). Peripheral spatial vision: Limits imposed by optics, photoreceptors, and receptor pooling. *Journal of Optical Society of America A*, *8*, 1775–1787.

Bedell, H. E. & Katz, L. M. (1982). On the necessity of correcting peripheral target luminance for pupillary area. *American Journal of Optometry and Physiological Optics*, *59*, 767–769.

Daitch, J. M. & Green, D. G. (1969). Contrast sensitivity of the human peripheral retina. *Vision Research*, *9*, 947–952.

De Vries, H. L. (1943). The quantum character of light and its bearing upon threshold of vision, the differential sensitivity and visual acuity of the eye. *Physica*, *X*, 553–564.

Enroth-Cugell, C. & Shapley, R. M. (1973). Flux, not retinal illumination, is what cat retinal ganglion cells care about. *Journal of Physiology*, *233*, 311–326.

Graham, N. & Hood, D. C. (1992). Quantal noise and decision rules in dynamic models of light adaptation. *Vision Research*, *32*, 779–787.

Kelly, D. H. (1972). Adaptation effects on spatio-temporal sine-wave thresholds. *Vision Research*, *12*, 89–101.

Koenderink, J. J., Bouman, M. A., Bueno de Mesquita, A. E. & Slappendel, S. (1978). Perimetry of contrast detection thresholds of moving spatial sine wave patterns. IV. The influence of the mean retinal illuminance. *Journal of Optical Society of America*, *68*, 860–865.

Laming, D. (1991). Contrast sensitivity. In Kulikowski, J. J., Walsh, V. & Murray, I. J. (Eds), *Limits of vision*. London: Macmillan.

Mandelbaum, J . & Sloan, L. L. (1947). Peripheral visual acuity. *American Journal of Ophthalmology*, *30*, 581–588.

Mustonen, J., Rovamo, J. & Näsänen, R. (1993). The effects of grating area and spatial frequency on contrast sensitivity as a function of light level. *Vision Research*, *33*, 2065–2072.

Mäkelä, P., Whitaker, D. & Rovamo, J. (1993). Modelling of orientation discrimination across the visual field. *Vision Research*, *33*, 723–730.

Näsänen, R., Kukkonen, H. & Rovamo, J. (1993). Spatial integration of band-pass filtered patterns in noise. *Vision Research*, *33*, 903–911.

Pelli, D. G. (1990). The quantum efficiency of vision. In Blakemore, C. (Ed.), *Vision: Coding and efficiency*. Cambridge: Cambridge University Press.

Pelli, D. G. & Zhang, L. (1991). Accurate control of contrast on microcomputer displays. *Vision Research*, *31*, 1337–1350.

Rose, A. (1942). The relative sensitivities of television pickup tubes, photographic film, and the human eye. *Proceedings of the Institute of Radio Engineers*, 293–300.

Rovamo, J. (1983). Cortical magnification factor and contrast sensitivity to luminance-modulated chromatic gratings. *Acta Physiologica Scandinavica, 119*, 365–371.

Rovamo, J. & Raninen, A. (1990). Cortical acuity and the luminous flux collected by retinal ganglion cells at various eccentricities in human rod and cone vision. *Vision Research, 30*, 11–21.

Rovamo, J. & Virsu, V. (1979). An estimation and application of the human cortical magnification factor. *Experimental Brain Research, 37*, 495–510.

Rovamo, J., Luntinen, O. & Näsänen, R. (1993a). Modelling the dependence of contrast sensitivity on grating area and spatial frequency. *Vision Research, 33*, 2773–2788.

Rovamo, J., Mustonen, J. & Näsänen, R. (1994). Modelling contrast sensitivity as a function of retinal illuminance and grating area. *Vision Research, 34*, 1301–1314.

Rovamo, J., Kukkonen, H., Tiippana, K. & Näsänen, R. (1993b). Effects of luminance and exposure time on contrast sensitivity in spatial noise. *Vision Research, 33*, 1123–1129.

Savage, G. L. & Banks, M. S. (1992). Scotopic visual efficiency: Constraints by optics, receptor properties, and rod pooling. *Vision Research, 32*, 645–656.

Van Nes, F.L. & Bouman, M. A. (1967). Spatial modulation transfer in the human eye. *Journal of the Optical Society of America, 57*, 401–406.

Van Nes, F. L., Koenderink, J. J., Nas, H. & Bouman, M. A. (1967). Spatiotemporal modulation transfer in the human eye. *Journal of the Optical Society of America, 57*, 1082–1088.

Virsu, V. & Rovamo, J. (1979). Visual resolution, contrast sensitivity, and the cortical magnification factor. *Experimental Brain Research, 37*, 475–494.

Wetherill, G. B. & Levitt, H. (1965). Sequential estimation of points on a psychometric function. *British Journal of Mathematical and Statistical Psychology, 18*, 1–10.

*Acknowledgements*—We thank the Academy of Finland, Ministry of Education, The Association of Finnish Ophthalmic Opticians, Information Centre of Optics Business and the Optics Division of Instrumentarium Corporation for support. Juvi Mustonen was supported by grants from the National Agency for Health and Welfare in Finland and the Association of Optometry in Finland. Risto Näsänen was supported by a Rosenberg's travel grant from the University of Helsinki.

## APPENDIX

*The least-square curves*

Contrast sensitivity as a function of retinal illuminance was modelled by fitting equation (2) to the contrast sensitivity data of Figs 1 and 2 at each spatial frequency and eccentricity separately. This was obtained by finding the minimum of the following:

$$G = \sum_{j=1}^{n} [(S_j^{-2} - k_1 - k_2/I_j)/S_j^{-2}]^2, \quad \text{(A1)}$$

where $k_1 = S_{\max}^{-2}$, $k_2 = I_c S_{\max}^{-2}$, and $S_j$ are contrast sensitivities corresponding to retinal illuminances $I_j$ in Figs 1 and 2. It is necessary to calculate the relative least-squares curves by minimizing the percentage error, as in equation (A1), because the range of $S_j^{-2}$ is several log units. Otherwise the deviations of the large values of $S_j^{-2}$ from the least-squares curve would dominate the fitting procedure. Equation (A1) was next transformed to

$$G = \sum_j [1 - k_1 S_j^2 - k_2 S_j^2/I_j]^2. \quad \text{(A2)}$$

The values of $k_1$ and $k_2$ that minimize $G$ were then found by the method described in Mäkelä, Whitaker and Rovamo (1993). Thereafter we calculated $S_{\max} = 1/\sqrt{k_1}$ and $I_c = k_2/k_1$.

*Explained variance*

The goodness of the fit of an equation to the data was estimated as follows: first we calculated error variance $n^{-1}\Sigma(\log Y - \log Y_{est})^2$ of the experimental data ($Y$) from the predicted values ($Y_{est}$) and the total variance $n^{-1}\Sigma(\log Y - Y_{ave})^2$ of the data, where $Y_{ave} = n^{-1}\Sigma \log Y$ is the average of log $Y$. The explained proportion was then calculated as:

$$r^2 = 1 - \sum(\log Y - \log Y_{est})^2 / \sum(\log Y - Y_{ave})^2. \quad \text{(A3)}$$

The values of $Y_{est}$ were calculated by means of equation (2). We used log $Y$ instead of $Y$, because $Y$ is plotted on a logarithmic scale. The explained proportion ($r^2$) is usually given as the percentage of the variance explained, which is obtained by multiplying the proportion by 100.